

# Dense Atom Clouds in a Holographic Atom Trap

R. Newell, J. Sebby, and T. G. Walker

*Department of Physics, University of Wisconsin-Madison, Madison, Wisconsin 53706*

(Dated: October 29, 2018)

We demonstrate the production of high density cold atom samples ( $2 \times 10^{14}$  atoms/cm<sup>3</sup>) in a simple optical lattice formed with YAG light that is diffracted from a holographic phase plate. A loading protocol is described that results in 10,000 atoms per lattice site. Rapid free evaporation leads to phase space densities of 1/150 within 50 msec. The resulting small, high density atomic clouds are very attractive for a number of experiments, including ultracold Rydberg atom physics.

PACS numbers: 1234567

Conventional light-force atom traps, in particular the magneto-optical trap (MOT), are limited in density by radiation trapping to typically  $10^{11}$  cm<sup>-3</sup> [1, 2]. In the experiments described here, we attain densities in far-off-resonance traps (FORTs) that exceed this density by 3 orders of magnitude, and are comparable to BEC densities. We show that FORTs can achieve these densities in tens of milliseconds, as compared to tens of seconds for magnetic traps. Such rapidly produced high density sources are of particular interest for studying novel collision phenomena that do not require the coherence of BECs and yet can be exploited for quantum manipulation and entanglement of atoms. They are also attractive for evaporative cooling; several groups have recently cooled atoms to quantum degeneracy using FORTs [3, 4].

FORTs [5] use spatially varying intensities  $I(\mathbf{r})$  to produce a conservative potential  $U(\mathbf{r}) = -2\pi\alpha(\lambda)I(\mathbf{r})/c$ , where  $\alpha(\lambda)$  is the polarizability of the atom at the FORT laser wavelength  $\lambda$ . At a given temperature  $T$  and number of trapped atoms  $N$  the peak density depends not directly on the trap depth but rather on its curvature:  $n \sim N(\kappa/T)^{3/2}$ , where  $\kappa = -\partial_{\mathbf{r}}^2 U$ . Therefore much higher densities can be obtained at roughly the same trap depth by forming an interference pattern (optical lattice) to obtain a rapid spatial variation in the intensity. In general, for a fixed laser power and beam area, forming an interference pattern (lattice) of cell size  $\Lambda$  from  $M$  beams increases the trap depth over a single-beam FORT by a factor  $O(M)$  and the spring constant by a factor  $O(M/\Lambda^2)$ . However, the number of atoms per lattice site is reduced by  $O(\Lambda^3)$  so that the geometrical factors cancel and the density scales as  $M^{3/2}$ . Thus there is considerable freedom in choosing the geometry of lattice FORTs without sacrificing density.

For phenomena occurring at high densities ( $> 10^{13}$  cm<sup>-3</sup>) it is desirable to construct a lattice FORT with sufficient unit cell volume that many atoms can be loaded into a given lattice site. This has been demonstrated by several groups using a variety of trap geometries: 3D lattice [6], crossed dipole [3], a single retro-reflected beam [4, 7], a beam focused with an array of microlenses [8], and the interference of light diffracted from a holographic phase plate [9]. All save the last two require interferometric stability and single-mode lasers. In an early experiment Boiron *et al.* used a holographic phase plate

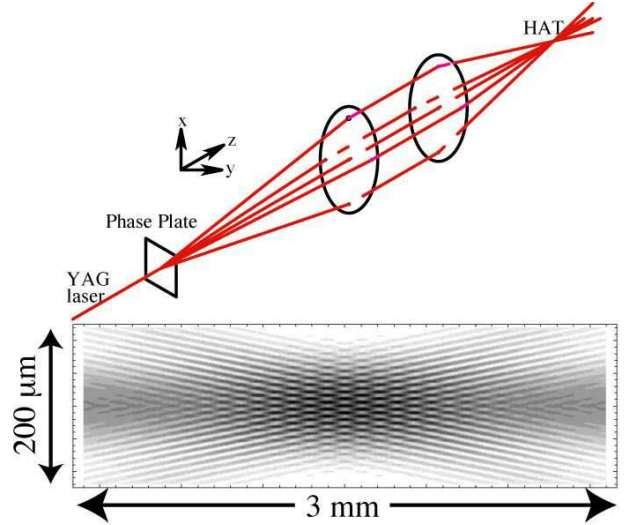


FIG. 1: Optical train used to produce the HAT, and calculation of the interference pattern formed at the intersection of the five HAT beams.

and a YAG laser to construct a large  $\Lambda$  Cs lattice. After applying blue Sisyphus cooling, they obtained densities of order  $10^{13}$  cm<sup>-3</sup>. In this work we use higher intensities, optimized loading, and evaporation without the aid of Sisyphus cooling to attain Rb densities exceeding  $10^{14}$  cm<sup>-3</sup> and phase space densities approaching 1/150 after loading for only tens of milliseconds. Furthermore our use of a multimode flashlamp-pumped laser demonstrates the robust nature of the trap.

In our experiments we use a YAG laser to achieve an optical lattice, called a Holographic Atom Trap (HAT), by interfering five diffracted beams from a holographic phase plate [10] (Fig. 1). At the intersection of the 5 laser beams an interference pattern

$$\frac{I(\mathbf{r})}{I_0} = \left| e^{ikz} + 2\beta e^{ikz(1-\theta^2/2)} (\cos kx\theta + \cos ky\theta) \right|^2 \quad (1)$$

is produced and Rb atoms ( $\alpha(1.06\mu\text{m}) = 105\text{\AA}^3$  [11, 12]) are trapped at the intensity maxima. Here  $k = 2\pi/\lambda$ ,  $\theta = 0.1$  rad is the diffraction angle of the four first-order beams,  $\beta^2 = 0.20$  is the ratio of the intensity of a single first-order diffracted beam to that of the zeroth order

beam  $I_0$ . Along the  $\hat{z}$  propagation direction of the light the interference arises from the Talbot effect[9]. The resulting lattice sites (microtraps) are  $10\ \mu\text{m} \times 10\ \mu\text{m} \times 100\ \mu\text{m}$  in size. With the individual beams focused to  $80\ \mu\text{m}$  and a total power of 8 W the depth of the central microtrap is  $500\ \mu\text{K}$  and the oscillation frequencies are 17 kHz, 17 kHz, and 0.7 kHz. These calculated frequencies were experimentally confirmed by parametric heating of the HAT atoms [7]. Since the lasers are nearly coprop-

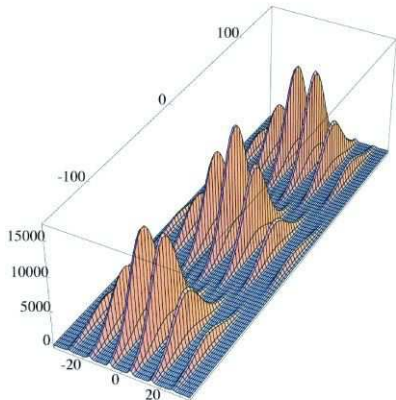


FIG. 2: Calculate density distribution of atoms in the HAT, assuming a Boltzmann distribution with a temperature equal to 1/10 the maximum trap depth. Distances are in microns, densities in arbitrary units.

agating, the potential is quite stable against vibrations and the YAG laser can have a large bandwidth. Our multi-longitudinal mode laser has a bandwidth of approximately 25 GHz. Heating due to intensity noise [13] was easily eliminated with an acousto-optic intensity stabilizer. The relatively large lattice sites allow many atoms ( $\sim 10^4$ ) to be trapped in each site.

Fig. 2 shows a calculated density distribution for atoms trapped in the HAT at  $50\ \mu\text{K}$  temperature. We use a probe laser propagating along the  $\hat{y}$ -direction to take spatial heterodyne [14] phase images that show the atoms' isolation within the Talbot fringes and the microtraps (Fig. 3). We observe Bragg diffraction of the probe beam from the atoms in the microtraps by interference with the probe beam, also shown in Fig. 3. An interesting observation from Fig. 2 is that there should be a relative misalignment of the microtraps in successive Talbot fringes. This is confirmed by the spatial profiles shown in Fig. 4. Analysis of such images gives about  $4 \times 10^5$  atoms per Talbot fringe. Time-of-flight temperature measurements of  $50\ \mu\text{K}$  coupled with knowledge of the trapping potential implies peak densities exceeding  $2 \times 10^{14}\ \text{cm}^{-3}$  and phase space densities of 1/150. Typically 25 microtraps are occupied within each Talbot fringe, with 10% of the atoms in the central microtrap.

Key to the HAT's success is an efficient loading protocol. We begin with a vapor cell forced dark spot MOT [15] with 50% of the  $10^7$  atoms in each of the hyper-

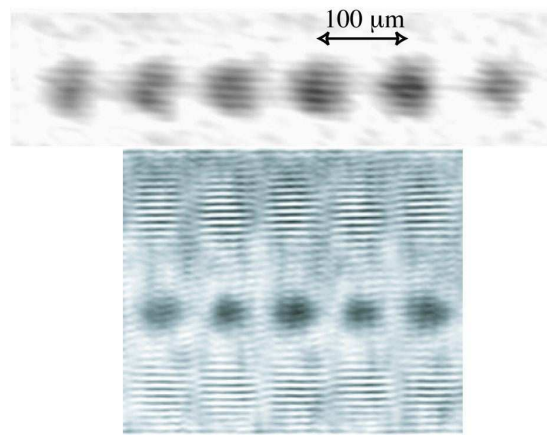


FIG. 3: Top: Image showing microtraps. Bottom: first order Bragg diffraction is shown in the fringes.

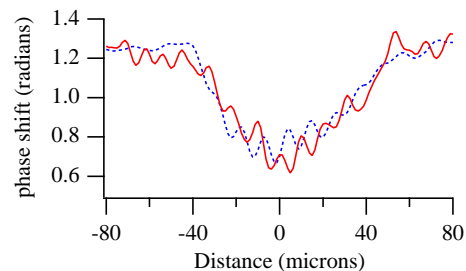


FIG. 4: Spatial profiles of two neighboring Talbot images. The microtrap structure is shifted between the two, as expected.

fine ground states ( $5S_{1/2}\ F=1,2$ ) of  $^{87}\text{Rb}$ . The dark spot is achieved by imaging an opaque object in the hyperfine repumping beam ( $F=1 \rightarrow 5P_{3/2}\ F'=2$ ). The trapping light ( $F=2 \rightarrow F'=3$ ) is tuned 3 linewidths  $\Gamma$  below resonance and has an intensity of  $72\ \text{mW}/\text{cm}^2$ . We add a depumping laser, tuned to the high frequency side of the  $F=2 \rightarrow F'=2$  resonance, to optically pump more atoms down to the  $F=1$  ground state. To load the HAT from the MOT, we compress the cloud by decreasing the trapping light intensity by a factor of 3, then increasing the MOT magnetic field. After 20 msec we turn on the HAT laser. AC Stark shifts tune the repumping and trapping beams away from resonance and the depumping beam towards resonance, causing the atoms in the HAT to be extremely dark (estimated  $\sim 0.001$  in  $F=2$  inside the FORT) [16]. During the HAT loading phase we shift the trapping laser detuning to  $-9\Gamma$ . The number of trapped atoms increases until it reaches steady state in about 50 msec, after which the MOT lasers are extinguished. The MOT to HAT transfer efficiency is as high as 15%.

We show in Fig. 5 the temperature and number of atoms vs time after the loading ceases. The temperature rapidly decreases to a value of about  $50\ \mu\text{K}$ , approximately 1/10 of the trap depth, as expected for free evaporation of atoms from the HAT [17]. The evapora-

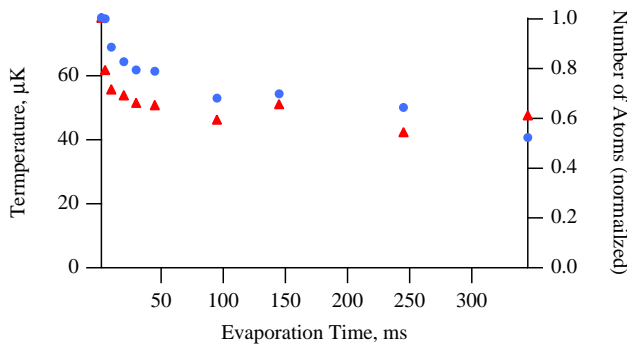


FIG. 5: Evaporative cooling of the atoms occurs after the cooling lasers are switched off. The number of atoms in a single Talbot fringe (circles) and the temperature (triangles) rapidly decrease until the temperature reaches roughly 1/10 the trap depth.

tion is rapid due to the very high densities; we estimate the elastic collision rate to exceed 3000/s. Such high collision rates make evaporative cooling very promising for the HAT and such experiments are underway in our laboratory. Trap lifetime studies show that after the evaporation ceases the temperature stays fixed but the atoms are slowly ejected from the trap and/or heated [18] by background gas collisions with a time constant of about 500 msec. For comparison, the MOT lifetime is typically

2-3 seconds for our vapor-loaded trap.

These high density samples are of potential interest for a variety of experiments. In addition to obvious examples such as evaporative cooling and cold collisions, many groups are interested in ultracold Rydberg atoms. Excitation of Rydberg states of principal quantum number  $\sim 100$  in our HAT will give rise to strong, long-range dipole-dipole interactions. Because atoms in our microtraps are localized within a  $15 \mu\text{m}$  region, these interaction energies are in excess of 1 MHz for atoms on opposite sides of a microtrap. Consequently, excitation by a narrow-band laser of more than one Rydberg atom at a time per microtrap should be greatly suppressed. This “dipole blockade” is of great interest for applications in quantum information processing [19] and single atom and photon sources [20]. Similarly, the densities are high enough to expect efficient excitation of novel long-range Rydberg molecules such as those recently proposed [21, 22]. In addition, it will be interesting to see how the very much higher densities achieved in the HAT as compared to MOTs affect the production of cold plasmas [23].

The authors are grateful for the support of NASA, the NSF, and the ARO. We thank Steve Kadlecik and Jason Day for pivotal contributions to the imaging system, and David Steele and Nathan Harrison for work on early stages of the experiment.

- 
- [1] T. Walker, D. Sesko, and C. Wieman, *Phys. Rev. Lett.* **64**, 408 (1990).
  - [2] W. Ketterle, K. Davis, M. A. Joffe, A. Martin, and D. E. Pritchard, *Phys. Rev. Lett.* **70**, 2253 (1993).
  - [3] M. D. Barrett, J. A. Sauer, and M. S. Chapman, *Phys. Rev. Lett.* **87**, 010404 (2001).
  - [4] S. R. Granade, M. E. Gehm, K. M. O’Hara, and J. E. Thomas, *Phys. Rev. Lett.* **88**, 120405 (2002).
  - [5] J. D. Miller, R. A. Cline, and D. J. Heinzen, *Phys. Rev. A* **47**, R4567 (1993).
  - [6] D. J. Han, S. Wolf, S. Oliver, C. McCormick, M. T. DePue, and D. S. Weiss, *Phys. Rev. Lett.* **85**, 724 (2000).
  - [7] S. Friebel, R. Scheunemann, J. Walz, T. W. Hansch, and M. Weitz, *Appl. Phys. B* **B67**, 699 (1998).
  - [8] R. Dumke, M. Volk, T. Muther, F. B. J. Buchkremer, G. Birkl, and W. Ertmer, *Phys. Rev. Lett.* **89**, 097903 (2002).
  - [9] D. Boiron, A. Michaud, J. M. Fournier, L. Simard, M. Sprenger, G. Grynberg, and C. Salomon, *Phys. Rev. A* **57**, R4106 (1998).
  - [10] MEMS Optical, Huntsville, AL.
  - [11] M. A. Kadar-Kallen and K. D. Bonin, *Phys. Rev. Lett.* **68**, 2015 (1992).
  - [12] M. Marinescu, H. R. Sadeghpour, and A. Dalgarno, *Phys. Rev. A* **49**, 5103 (1994).
  - [13] M. E. Gehm, K. M. O’Hara, T. A. Savard, and J. E. Thomas, *Phys. Rev. A* **58**, 3914 (1998).
  - [14] S. Kadlecik, J. Sebby, R. Newell, and T. G. Walker, *Opt. Lett.* **26**, 137 (2001).
  - [15] M. H. Anderson, W. Petrich, J. R. Ensher, and E. A. Cornell, *Phys. Rev. A* **50**, R3597 (1994).
  - [16] S. J. M. Kuppens, K. L. Corwin, K. W. Miller, T. E. Chupp, and C. E. Wieman, *Phys. Rev. A* **62**, 013406 (2000).
  - [17] K. M. O’Hara, M. E. Gehm, S. R. Granade, and J. E. Thomas, *Phys. Rev. A* **64**, 051403 (2001).
  - [18] S. Bali, K. M. O’Hara, M. E. Gehm, S. R. Granade, and J. F. Thomas, *Phys. Rev. A* **60**, R29 (1999).
  - [19] M. D. Lukin, M. Fleischhauer, R. Cote, L. M. Duan, D. Jaksch, J. I. Cirac, and P. Zoller, *Phys. Rev. Lett.* **87**, 037901 (2001).
  - [20] M. Saffman and T. G. Walker, *quant-ph/0203080* (2002).
  - [21] C. H. Greene, A. S. Dickinson, and H. R. Sadeghpour, *Phys. Rev. Lett.* **85**, 2458 (2000).
  - [22] C. Boisseau, I. Simbotin, and R. Cote, *Phys. Rev. Lett.* **88**, 133004 (2002).
  - [23] T. C. Killian, M. J. Lim, S. Kulin, R. Dumke, S. D. Bergeson, and S. L. Rolston, *Phys. Rev. Lett.* **86**, 3759 (2001).